CLEARINGHOUSE FOR FEDERAL SCIENTIFIC AND TECHNICAL INFORMATION CFSTI
DOCUMENT MANAGEMENT BRANCH 410.11

LIMITATIONS IN REPRODUCTION QUALITY

ACCESSION # AD 609030

☑ 1. WE REGRET THAT LEGIBILITY OF THIS DOCUMENT IS IN PART UNSATISFACTORY. REPRODUCTION HAS BEEN MADE FROM BEST AVAILABLE COPY.

☐ 2. A PORTION OF THE ORIGINAL DOCUMENT CONTAINS FINE DETAIL WHICH MAY MAKE READING OF PHOTOCOPY DIFFICULT.

☐ 3. THE ORIGINAL DOCUMENT CONTAINS COLOR, BUT DISTRIBUTION COPIES ARE AVAILABLE IN BLACK-AND-WHITE REPRODUCTION ONLY.

☐ 4. THE INITIAL DISTRIBUTION COPIES CONTAIN COLOR WHICH WILL BE SHOWN IN BLACK-AND-WHITE WHEN IT IS NECESSARY TO REPRINT.

☐ 5. LIMITED SUPPLY ON HAND: WHEN EXHAUSTED, DOCUMENT WILL BE AVAILABLE IN MICROFICHE ONLY.

☐ 6. LIMITED SUPPLY ON HAND: WHEN EXHAUSTED DOCUMENT WILL NOT BE AVAILABLE.

☐ 7. DOCUMENT IS AVAILABLE IN MICROFICHE ONLY.

☐ 8. DOCUMENT AVAILABLE ON LOAN FROM CFSTI (TT DOCUMENTS ONLY).

☐ 9.

PROCESSOR:

V. Ritenour

TSL-107-10/64

0 25

DEPARTMENT OF ELECTRICAL ENGINEERING

UNIVERSITY OF UTAH

SALT LAKE CITY, ~~UTAH~~

AD 609030

Penetration and Cratering Study
Air Force Ballistic Missiles Division
12 Contract No. AF 04(647)-176

13 NA

14 Uncl.

6 PERFORATION OF THIN ALUMINUM TARGETS

by

8 Charles R. Morris, Wm. S. Partridge,
and Emerson T. Cannon

7 NA

11 Technical Report UU-1

10 43 p. incl.
illus. tables

9 August 1958

ABSTRACT

Steel spheres were accelerated to a velocity in the range between 0.5 km/sec to 2.63 km/sec and were impinged normally upon thin targets of aluminum. The amount of energy lost by a pellet in perforating a target was found to be directly proportional to the kinetic energy of the impinging pellet. The minimum amount of energy required for a pellet to perforate Al was found to be an increasing function of target thickness. It was also found that the hole diameter increased as the impact velocity increased.

TABLE OF CONTENTS

INTRODUCTION

The purpose of this report was to determine how much energy a small pellet lost in perforating a thin target and the minimum amount of energy of perforation. This information could be of use for example in regard to collisions between satellites and meteorites. It is theorized[1] that a meteorite is made of a low-strength material and upon impact with a surface will break up into many pieces which will, in turn, perforate the surface as small fragments.

If a high velocity pellet comes in contact with the surface, it causes an impulsive loading condition to exist on the target. An impulsive load is characterized by an almost instantaneous rise in load to a quite high but finite value which is followed immediately by a rapid decrease in load[2]. The distribution of the stresses established by an impulsive load will generally be transient and highly localized. Impulsive loading is very difficult to analyze since static methods are not applicable.

This report discusses experimental results obtained in regard to the energy lost by a pellet in a target and the minimum energy required for perforation. An attempt is also made to theoretically predict how the force on the target varies as a function of velocity.

---

[1] Baldwin, R. B. "The Face of the Moon", University Press, page viii and page 68.

[2] Rinehart, J. S. and Pearson, J. "Behavior of Metals Under Impulsive Loads", American Society of Metals, Cleveland, Ohio (1954).

EXPERIMENTAL PROCEDURE

Figure 1 shows the system used for this investigation. The foils were one mil thick and were made out of Mylar[3]. They were used in conjunction with the velocity measuring system. The target was made of aluminum 2024-T4 from thicknesses of 1/16, 1/8, 1/4, and 5/16 inch. A steel pellet having a diameter of 3/32 inch and a mass of 55 milligrams was used.

Acceleration of the Pellet

A special gun for the acceleration of the pellet was used. It consisted of two sections, each 24 inches long, which were bolted together. It had a smooth bore of .218 inch in diameter and was chambered to fire a 220 swift cartridge.

In order to avoid mass loss, the pellet was accelerated in a sabot[4]. The sabot was made of Texilite with an outside diameter equal to that of the bore. It consisted of two halves with the nose drilled to the same size of that of the pellet. The pellet was held in place by a small coating of vaseline. After leaving the muzzle of the gun, the two halves were forced apart by the air and the pellet was free to continue on.

Velocity Measurements

Each foil acted as a relay which was normally open, but could be closed by perforating the foil. Referring to Fig. 1, when the pellet

---

[3]Fullmer, M. D., Masters Thesis (1958).

[4]Partridge, W. S., Vanfleet, H. B., and Whited, C. R., Technical Report No. OSR-9.

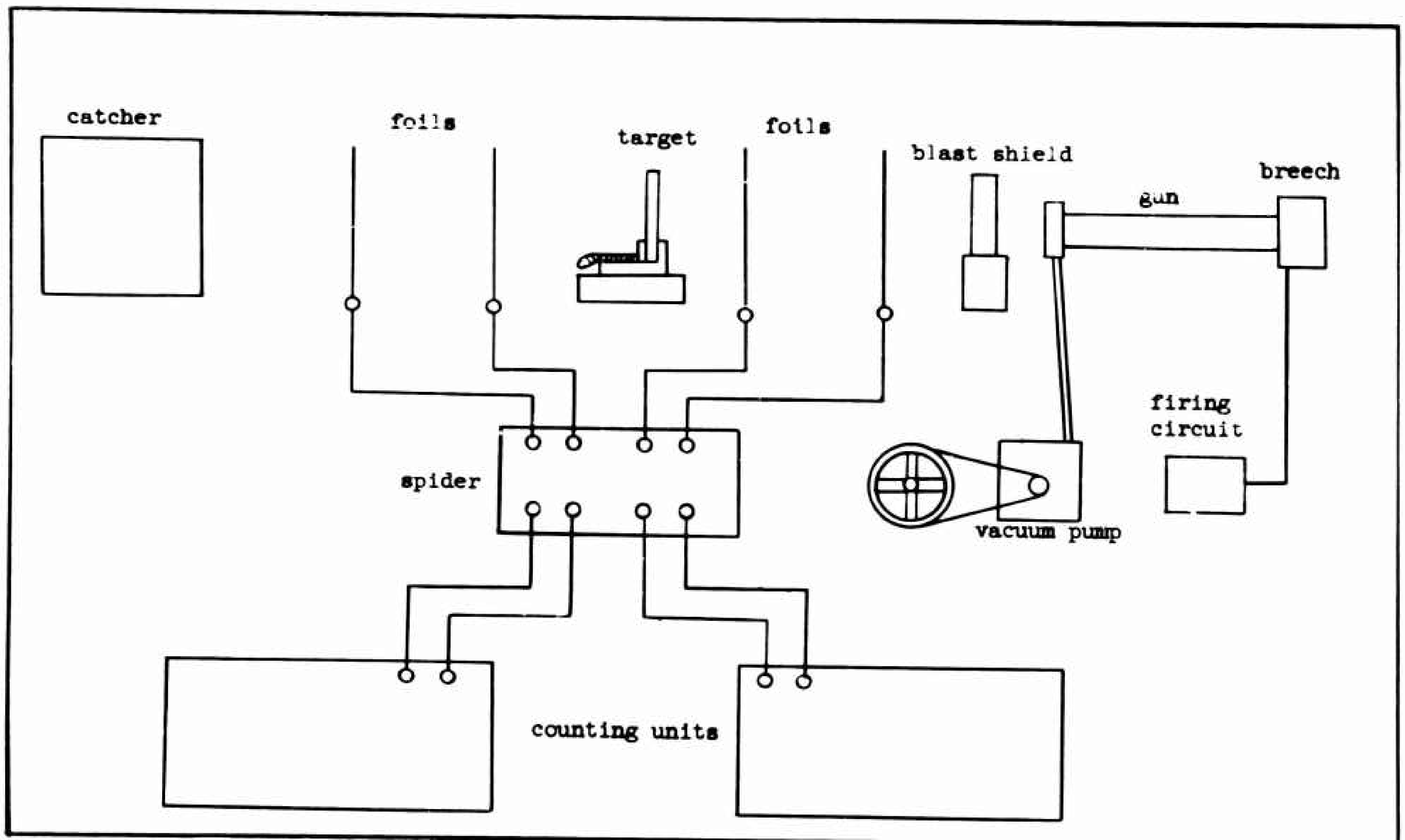

Fig. 1. Block Diagram of Test Setup

pellet perforated the first foil, a capacitor in the spider[5] discharged across a resistor causing a voltage pulse to start the counting unit. The counting unit was stopped in the same manner by foil two. The distance between the first and second foils was 50 cm. Knowing the distance and time, the impact velocity V_i was found. The exit velocity V_o was found in exactly the same manner as the impact velocity. The amount of energy lost by a pellet in a target is then given by

$$E_{lost} = \frac{1}{2} m_p (V_i^2 - V_o^2) \qquad (1)$$

where

m_p = mass of the pellet

V_i = velocity of the pellet prior to striking the target

V_o = velocity of the pellet after perforating the target

Two different types of counting units were used as a check against each other. Those used were two electronic counters and one Tektronix oscilloscope with dual sweeps. Figure 2 shows a photograph of the original equipment used.

Pellet and Hole Diameter Measurements

Measurements of pellet and hole diameters were made with a cathotometer, which is shown in Fig. 3. The distance between two points was measured by placing the internal hairline first on one point and then the other, recording the two corresponding readings

[5] See footnote 3, page 2.

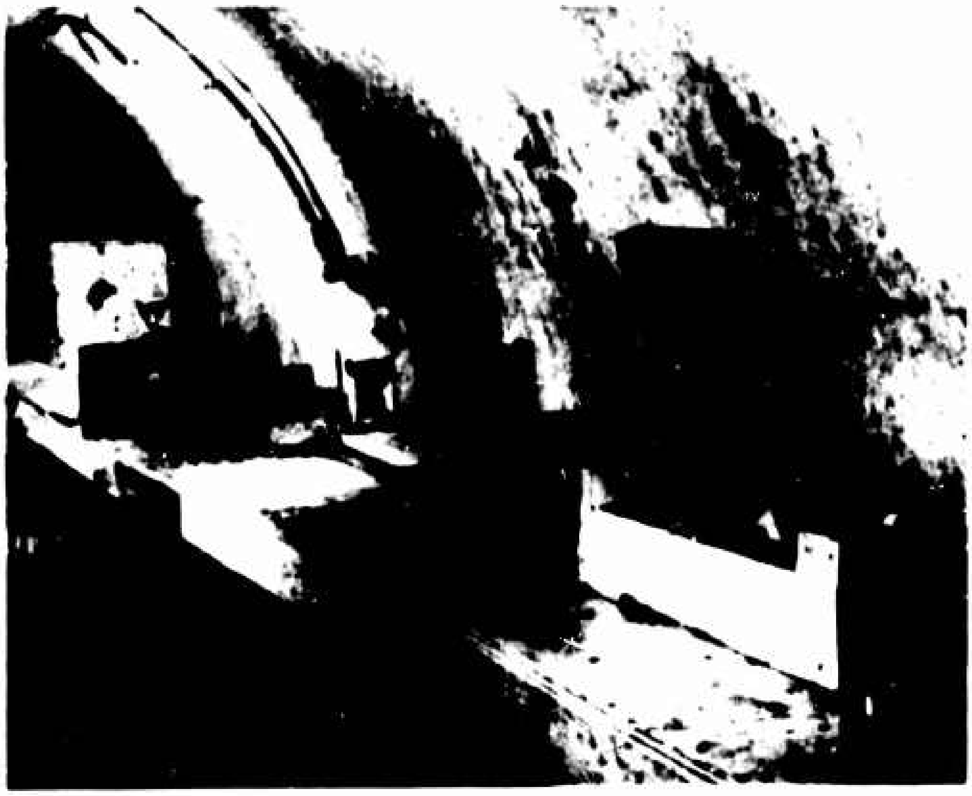

Fig. 2. Photograph of original setup

Fig. 3. Cathotometer used for measuring hole and pellet diameters

on the centimeter scale. The difference of these two readings was the distance.

PRESENTATION OF RESULTS

Pellets were accelerated to a velocity in the range between 0.5 and 2.6 km/sec and were impinged upon targets of Al 2024-T4. The amount of energy lost was calculated from Eq. 1 and a relationship of energy lost as a function of impact velocity was plotted in Figs. 4, 5, and 6.

In Figs. 4, 5, and 6, the ratio of energy lost to impact velocity increases as impact velocity is increased. A factor which could have influenced this was pellet deformation. In order to verify whether or not pellet deformation was a factor, pellets were caught at various velocities. It was found that the pellets deformed as impact velocity was increased. Figures 7, 8, and 9 show pellets which have perforated targets and the corresponding hole which they made.

In order to reach some conclusion, tungsten pellets were used to perforate the targets. It was hoped that the tungsten pellets would <u>not</u> deform upon perforating the target. The purpose of using tungsten was to be able to take the following ratio as a function of impact velocity:

$$\frac{E_{lost} \text{ (due to steel pellets, } \underline{\text{deformed}}\text{)}}{E_{lost} \text{ (due to tungsten pellets, } \underline{\text{not deformed}}\text{)}} \qquad (2)$$

If the ratio in Eq. 2 was found to be constant as impact velocity varied from 0.5 to 2.6 km/sec, the conclusion would have been that

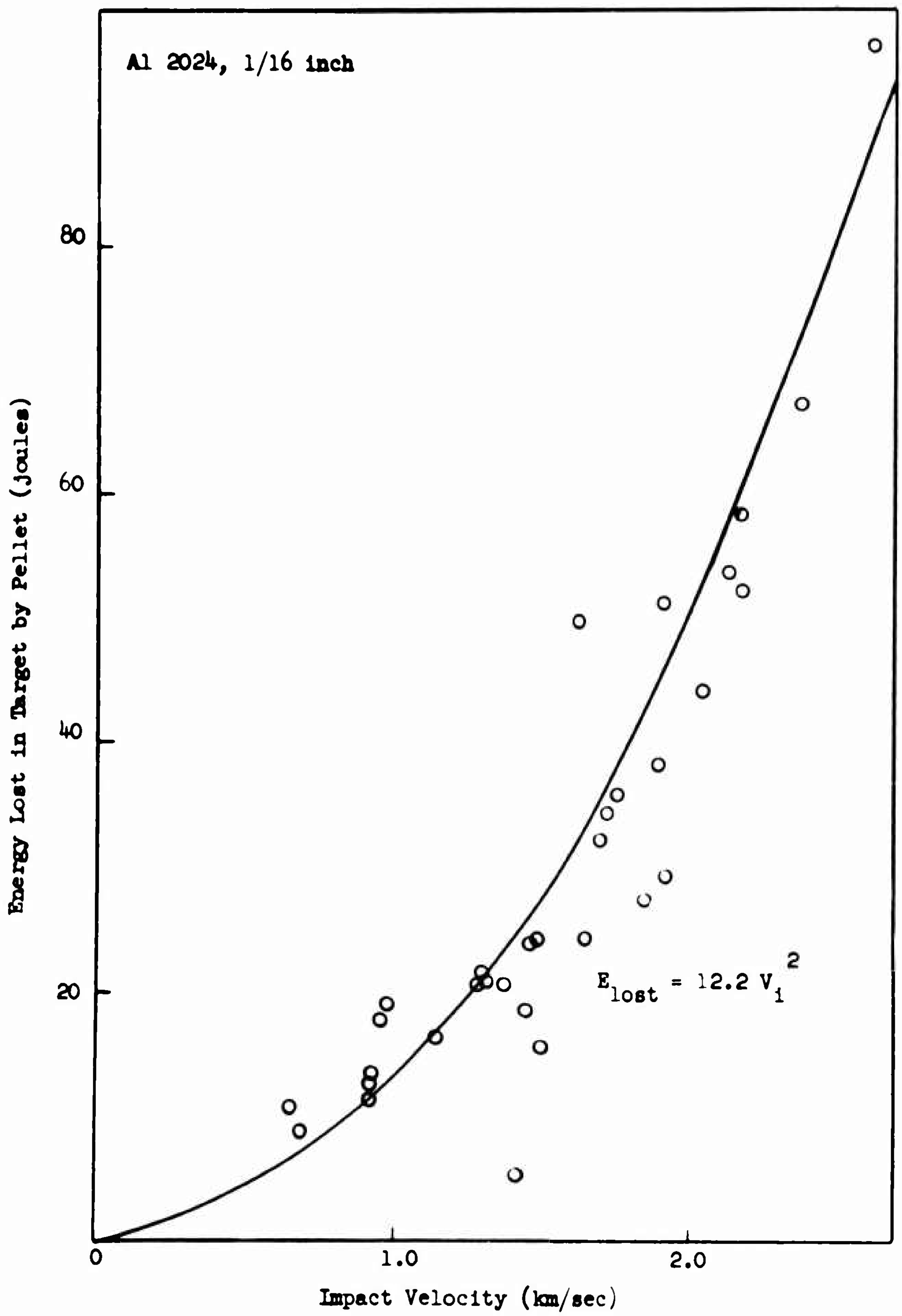

Fig. 4. Energy lost vs. impact velocity

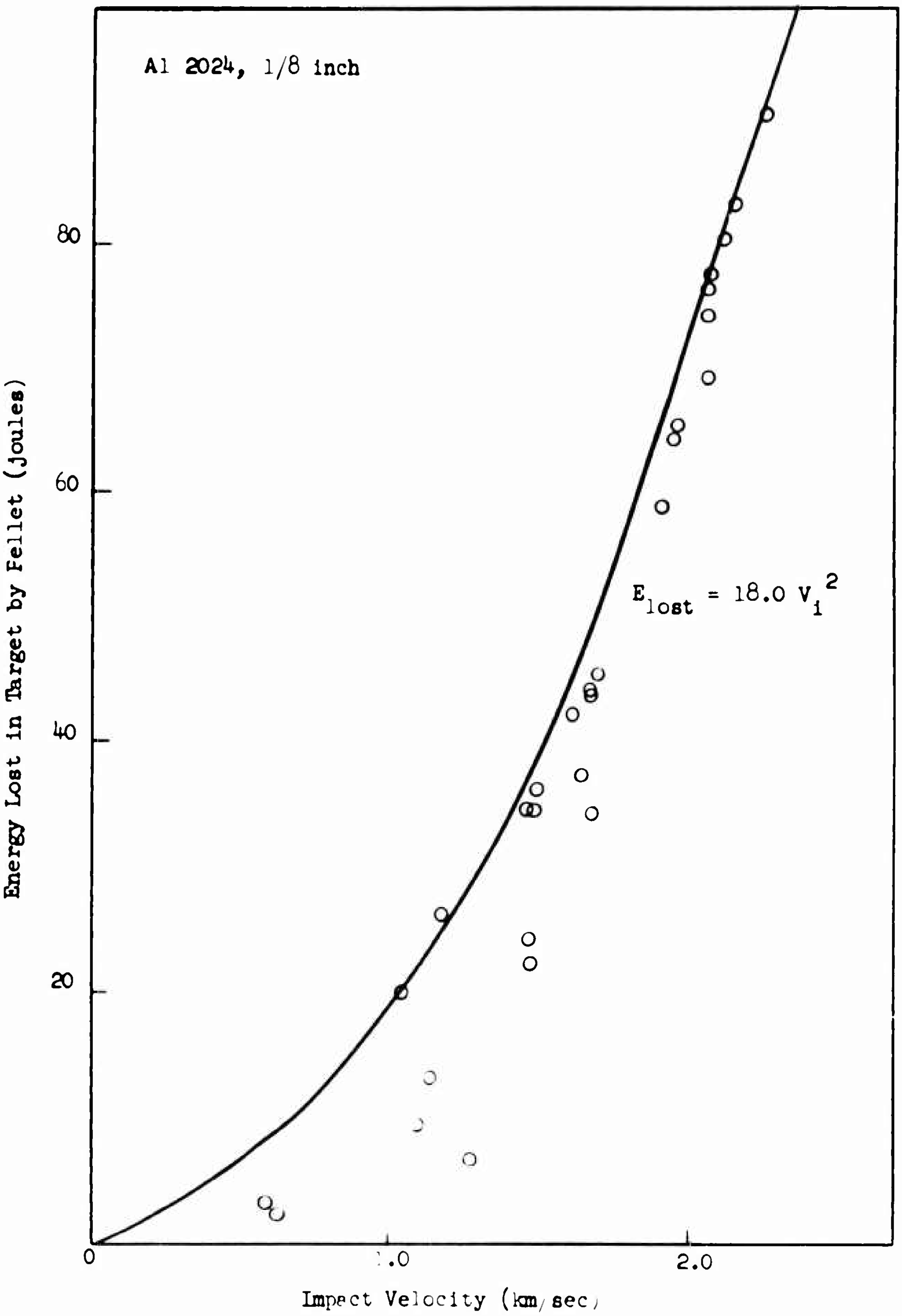

Fig. 5. Energy lost vs. impact velocity

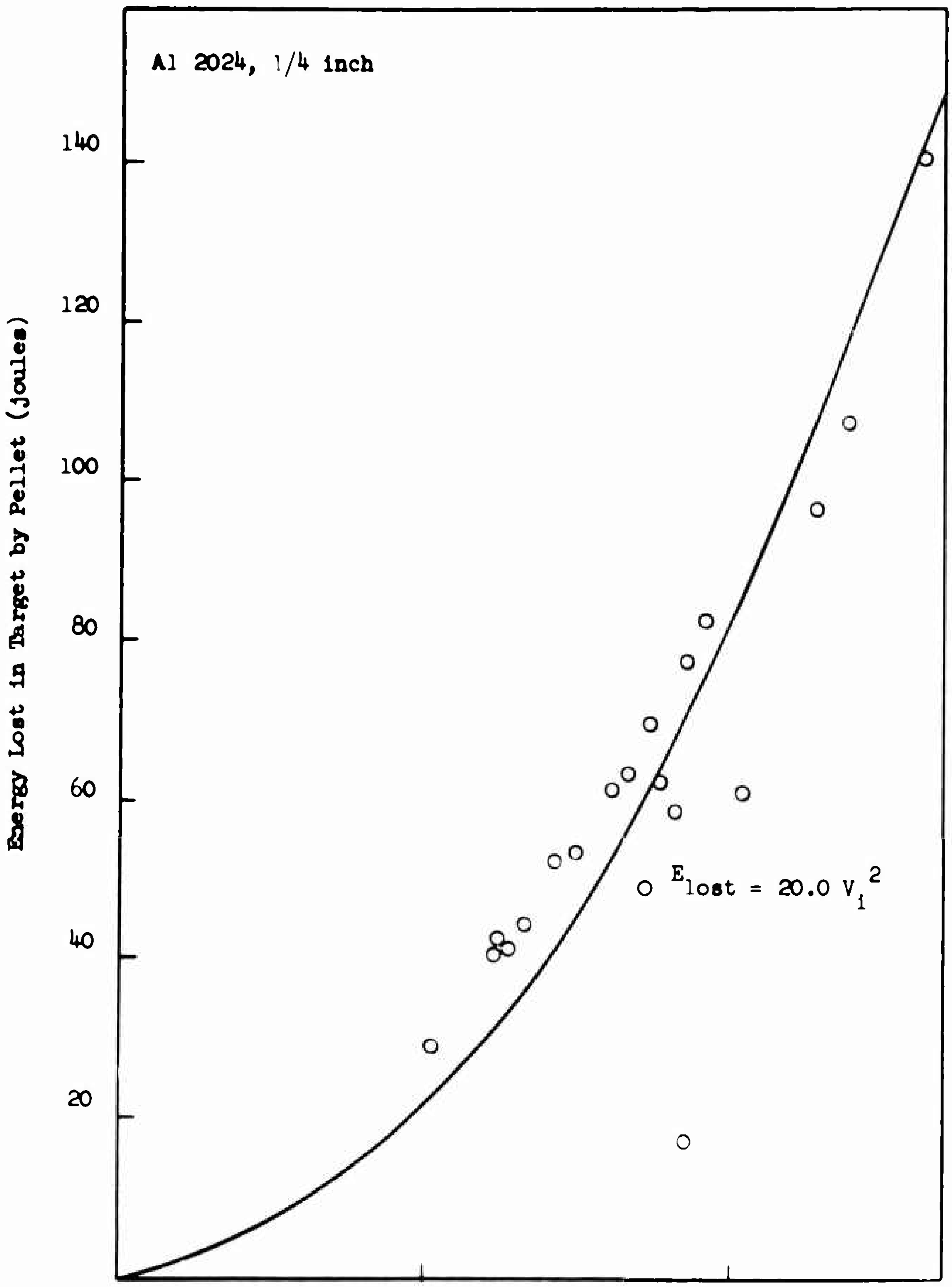

Impact Velocity (km/sec)

Fig. 5. Energy Lost vs. Impact Velocity

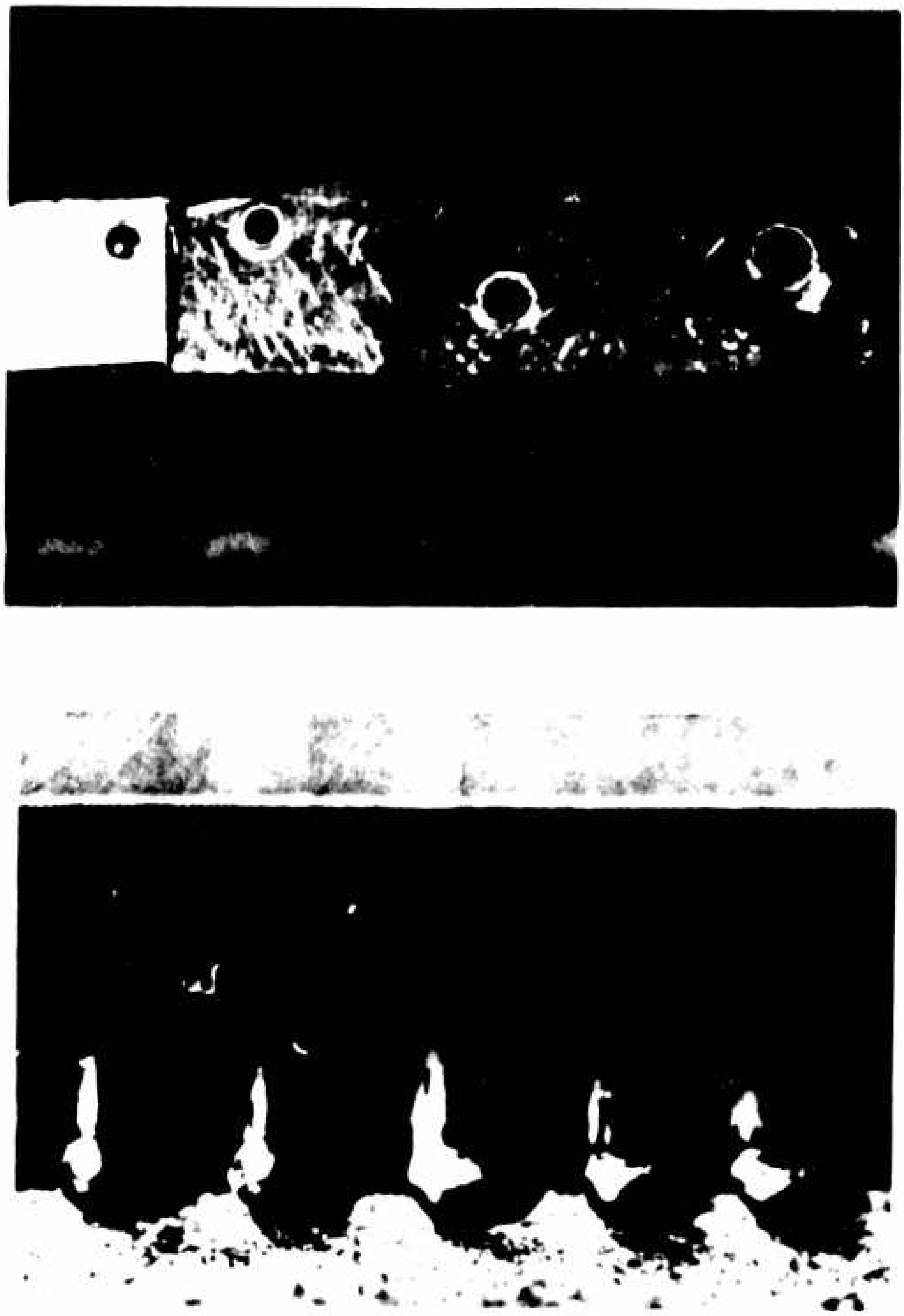

Fig. 7. Holes made in 1/16-inch Al by above pellets in order of increasing velocity from left to right

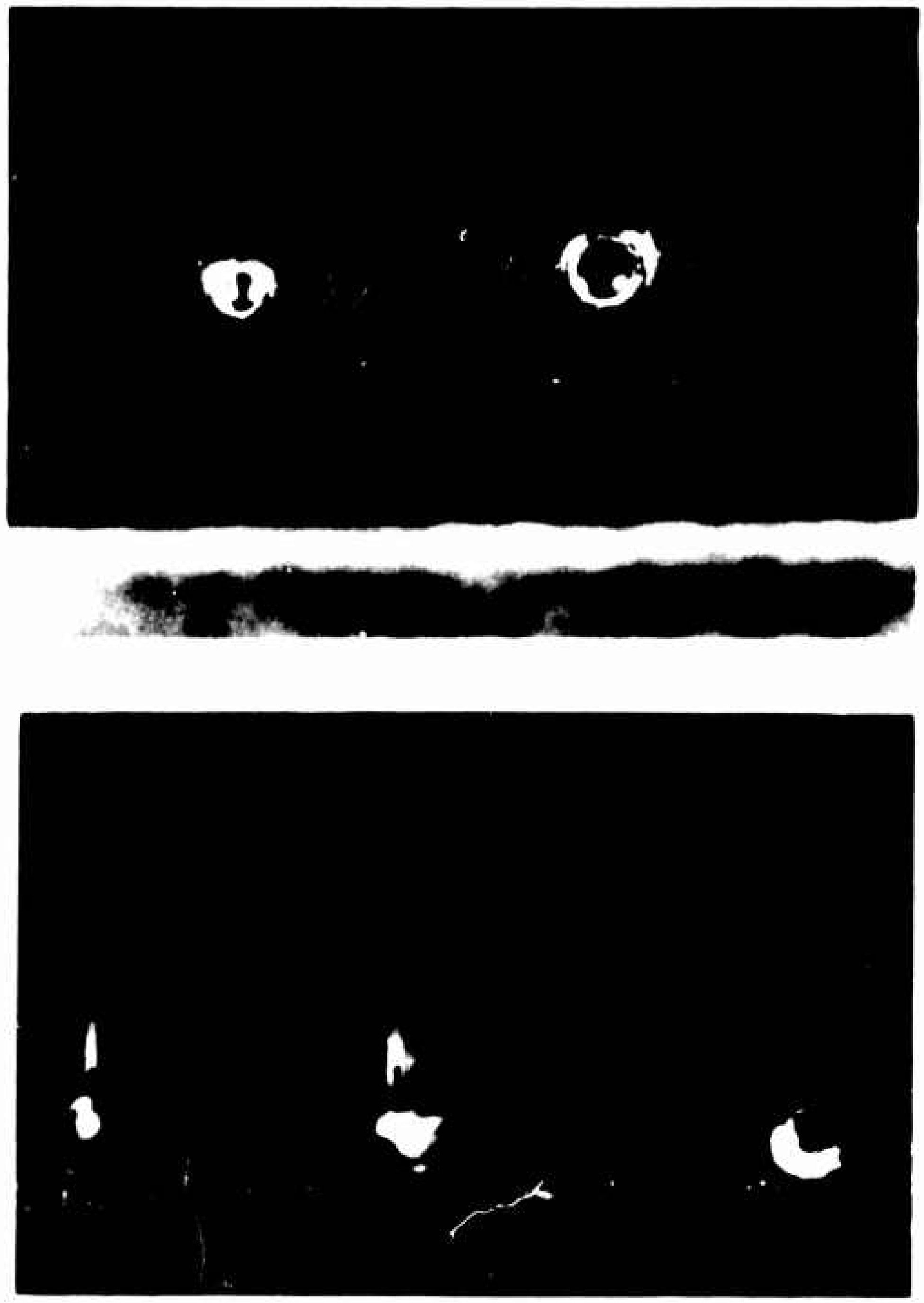

Fig. 8. Holes made in 1/8-inch Al by above pellets in order of increasing velocity from left to right

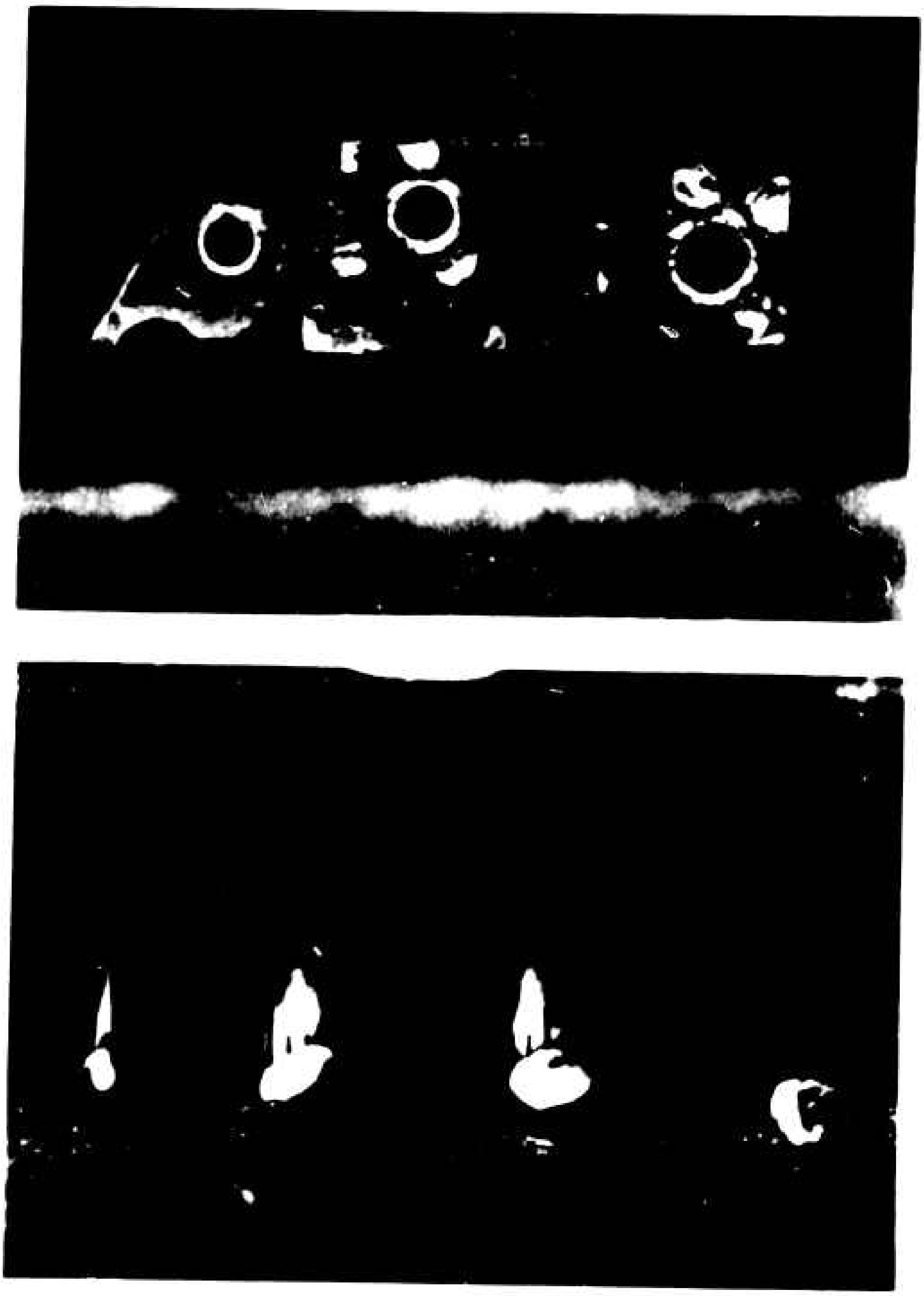

Fig. 9. Holes made in 1/4-inch Al by above pellets in order of increasing velocity from left to right

additional energy lost at higher velocities was not due to the deformation of the pellet. The tungsten pellets, however, disintegrated upon impact at high velocities, and no conclusion could be reached.

In order to determine how energy lost varied as a function of the kinetic energy of the pellet, curves were fitted to the points in Figs. 4, 5, and 6. A curve-fitting technique called the method of averages was used. Table I lists the curves found by this method.

Table I

Target Thickness (inches)	$E_{lost} = KV_i^n$ (joules)
1/16	$E_{lost} = 12.2\ V_i^{2.0}$
1/8	$E_{lost} = 18.0\ V_i^{1.9}$
1/4	$E_{lost} = 27.0\ V_i^{1.6}$

The curves in Table I show that for 1/16- and 1/8-inch targets, the energy lost is approximately a function of impact velocity squared. Since no exact method was available for relating the energy lost to impact velocity, the assumption was made that the energy lost varied as a function of impact velocity squared given by

$$E_{lost} = KV_i^2 \tag{3}$$

where

K = a different coefficient for each target thickness

Values of K were found such that an optimum fit existed between the curves and the points shown in Figs. 4, 5, and 6. It appeared that these curves satisfactorily described the energy lost as a function of impact velocity, and the assumption previously made was correct.

It is possible, however, that the exponent is a function of target thickness. Since the kinetic energy is given by $0.5\, m_p\, V_i^2$, a direct relationship can now be found between the energy lost and the kinetic energy of the pellet. This is given by

$$\frac{E_{impact}}{E_{lost}} = \frac{0.5\, m_p V_i^2}{K\, V_i^2} = \frac{m_p}{2K} \tag{4}$$

In order to determine the minimum energy needed to perforate aluminum, steel pellets were accelerated to a velocity which enabled them to be able to protrude through the back of the target. Figure 10 shows a front and back view of a 1/16-inch aluminum target used for determining the minimum energy of perforation.

Fig. 10. Front (left) and back (right) views of 1/16-inch aluminum used for minimum perforation test

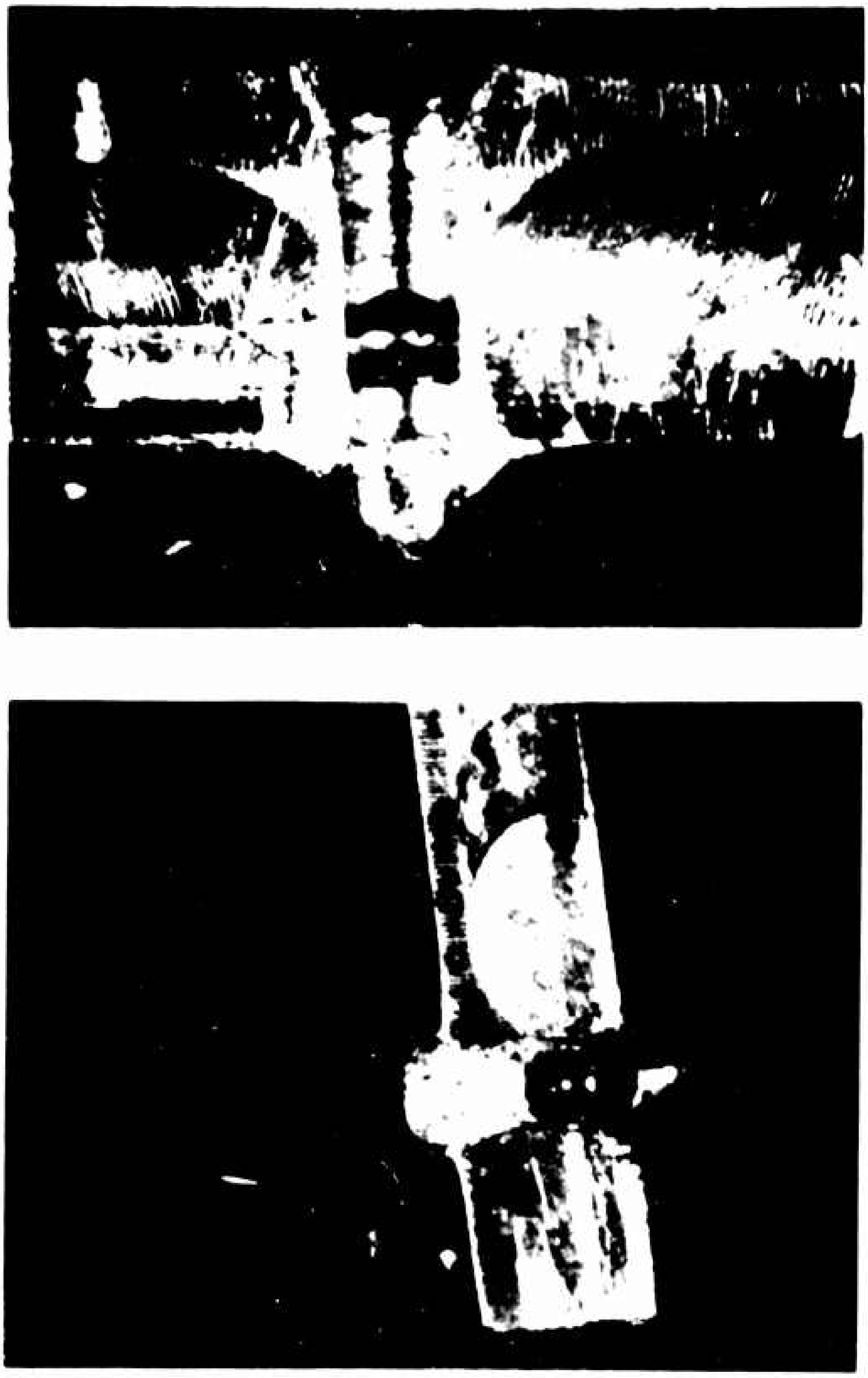

Fig. 11. Cross-sectional view of 5/16-inch Al penetrated by steel pellet

The hole marked 33 (see arrow) shows the pellet protruding through the back of the target. The back view also shows other holes which have been perforated or else which have only been penetrated.

Figure 11 shows two cross-sectional views of 5/16-inch aluminum which was penetrated by a steel pellet having a velocity of 1.87 km/sec. The markings were made by a milling machine which was used to cut down to the crater, pellet, and punchout. This photograph shows how the pellet has been deformed as it sheared out the aluminum in the form of a punchout.

A plot of minimum energy of perforation as a function of target thickness is shown in Fig. 12. Table II also shows a comparison of the energy, velocity, and thickness.

Table II

Target Thickness (inches)	V_{min} (km/sec)	E_{min} (joules)
1/16	0.417	4.8
1/8	0.816	18.3
1/4	1.200	39.6
5/16	1.870	97.4

No suitable curve could be found which would fit these points. Fig. 12 does show, however, that the minimum energy of perforation is an increasing function of target thickness.

Using the cathotometer, hole diameters and pellet thickness were measured. Pellet thickness means the distance from the back of the pellet to the front side which was flattened by impact. Except for

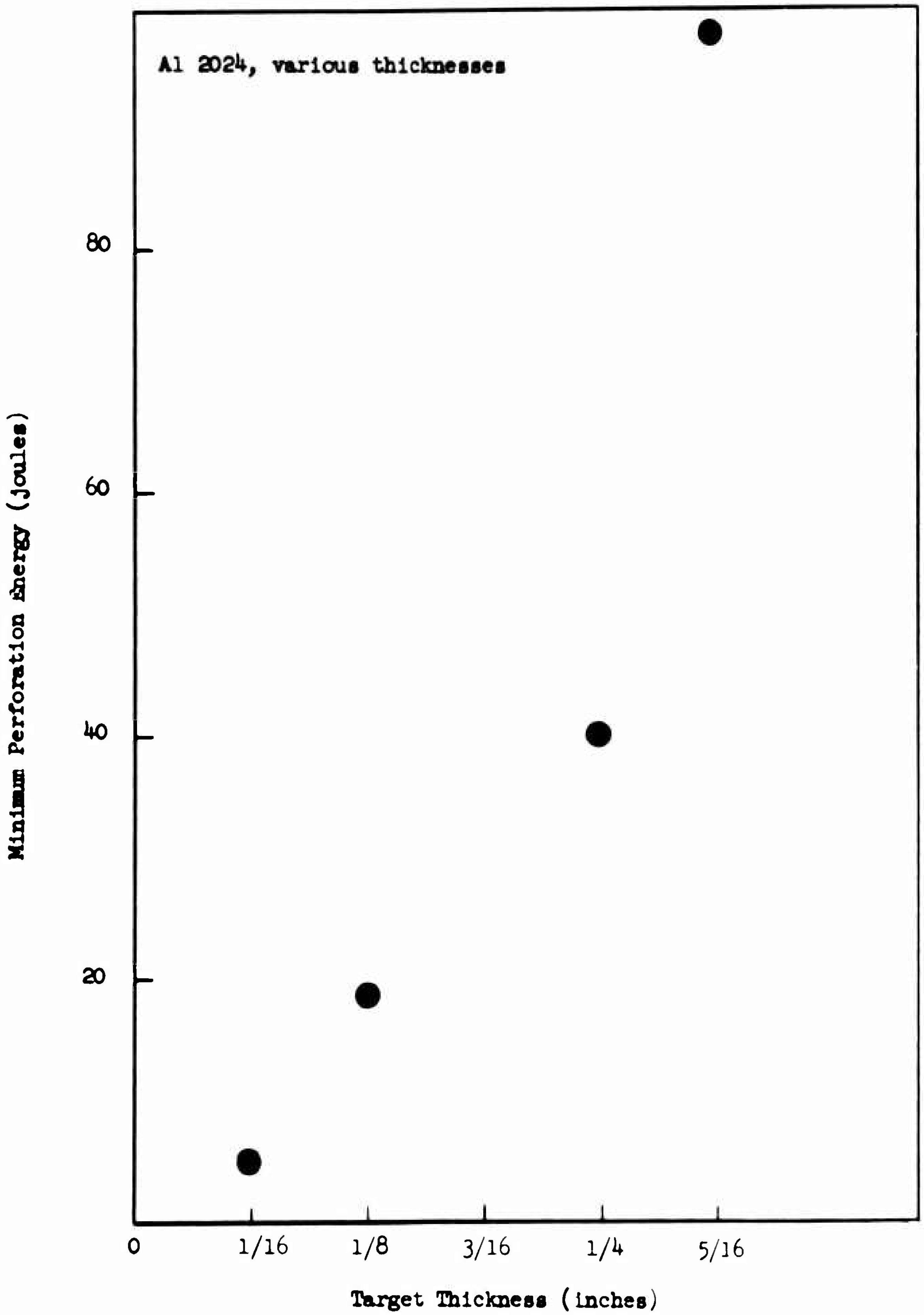

Fig. 12. Minimum perforation energy vs. thickness

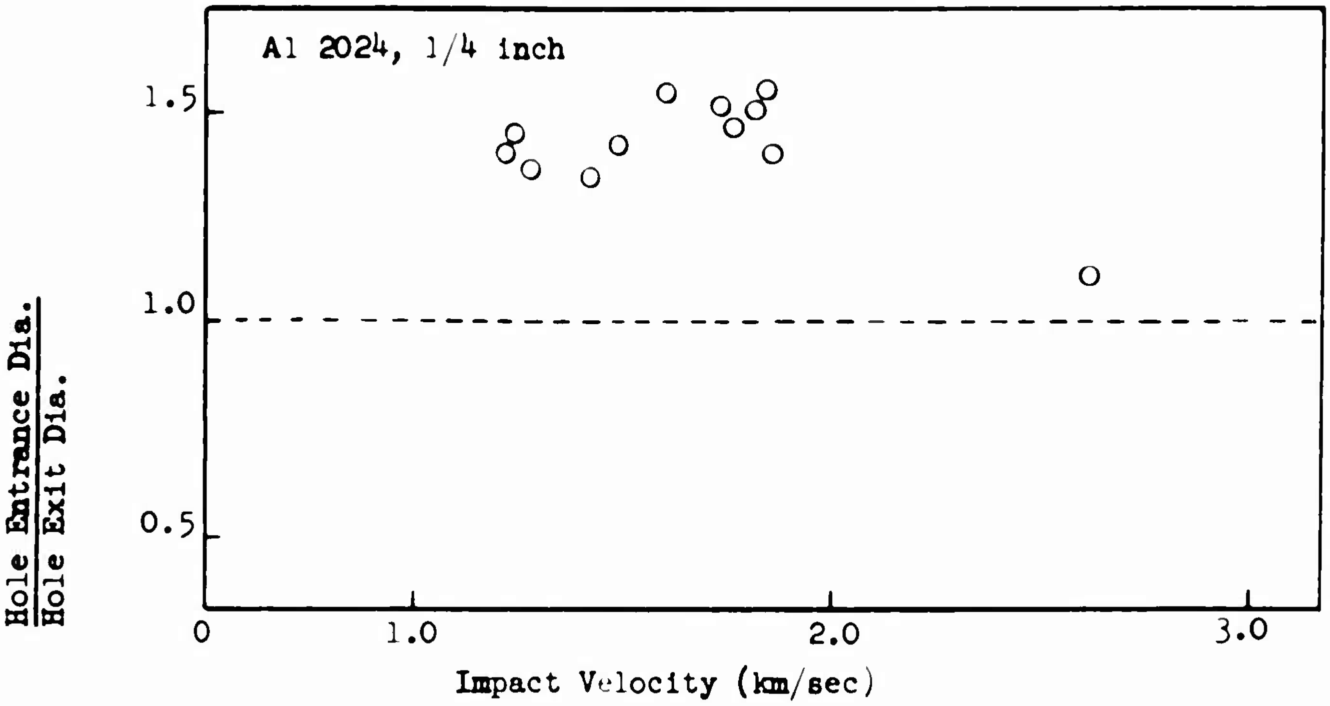

Fig. 13. Comparison of hole diameters vs. impact velocity

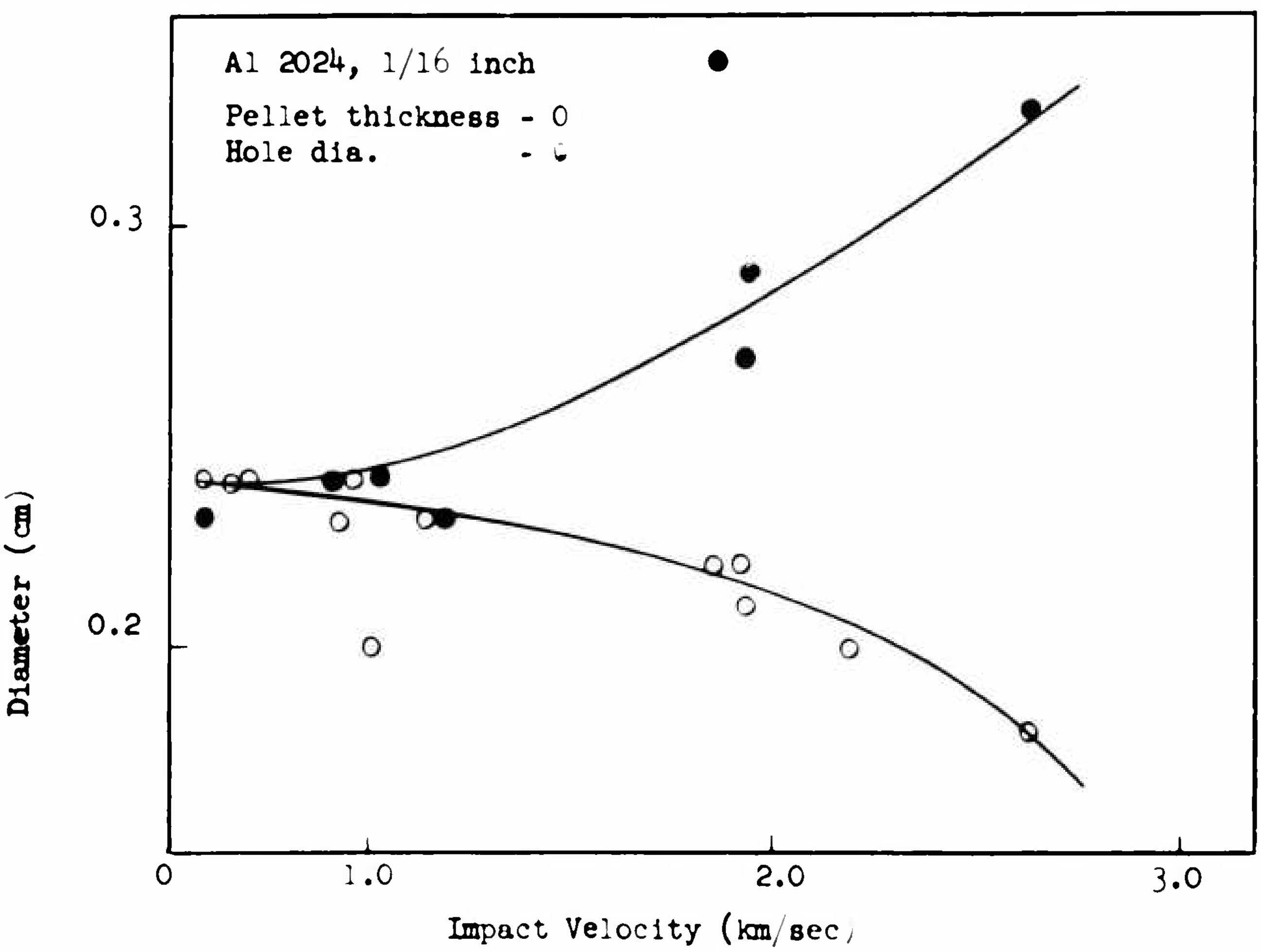

Fig. 14. Pellet thickness and hole dia. vs. impact velocity

1/4-inch targets, there wasn't much distinction between the entrance and exit diameters of the holes. Figure 13 shows a comparison of hole entrance diameter to hole exit diameter as a function of impact velocity.

Figure 14 shows how the average hole diameter increases as the pellet becomes more flat with an increase in velocity.

DISCUSSION OF RESULTS

Energy Lost by Pellet

It has been found that the energy lost by a pellet as a function of impact velocity can be described by

$$E_{lost} = KV_1^{\;2} \tag{3}$$

where

K = 12.2 for 1/16-inch targets
18.0 for 1/8-inch targets
20.0 for 1/4-inch targets

It was also found that the relation between energy lost and the kinetic energy of the pellet was given by

$$\frac{E_{impact}}{E_{lost}} = \frac{m_p}{2K} \tag{4}$$

Equation 4 shows the amount of energy lost by a pellet in a thin target of aluminum is directly proportional to the kinetic energy of the impinging pellet.

In order to predict the energy lost for any thickness between 1/16 and 5/16 inch, a nomograph is shown in Fig. 15. To use the

Fig. 15. Nomograph for relating thickness, impact velocity, and energy lost

nomograph, place the edge of a straight edge on the particular thickness desired and also on the desired impact velocity. The energy lost is then read directly from the chart.

Minimum Perforation Energy

In Fig. 12 it appears that the ratio of minimum perforation energy to target thickness is an increasing function of thickness. One reason for this might be due to the deformation of the pellets. It has also been suggested that a fluid state might be reached by the pellet where it begins to melt and the mass decreases. If this were true, a higher velocity would be needed to cause perforation. Since energy is proportional to mass and the square of velocity, a decrease in mass and increase in velocity would mean a probable increase in energy.

Hole Size as a Function of Energy

It was found that as the energy of the pellet was increased, the hole size increased. This is shown in Fig. 14. Figure 16 shows a photograph of 1/4-inch aluminum which has been perforated by a pellet traveling at 1.2 km/sec and then at 2.17 km/sec. The diameter of the small hole was the same diameter as the pellet, whereas, the larger hole had a diameter of approximately twice that of the pellet. It has already been established that the volume of a crater is directly proportional to the kinetic energy of the pellet[6].

It was also found that the appearance of the hole went from a cone to a cylinder as impact velocity was increased. This is shown in Fig. 13.

---

[6] See footnote 4, page 2.

Linear Momentum of Pellet

In Figs. 4, 5, and 6, the energy lost as a function of impact velocity can, in general, be described by:

$$m_p \left(V_i^2 - V_o^2\right) = k_1 V_i^2 \qquad (5)$$

where

k_1 = 2 K, where K is a particular coefficient for a particular thickness of aluminum

V_i = impact velocity of pellet

V_o = exit velocity of pellet after perforating target

Fig. 16. Left view shows hole made by low velocity pellet
Right view shows hole made by high velocity pellet

The change in linear momentum of the pellet can be found from Eq. 5 as

$$m\Delta v = \frac{k_1 V_i^{\,2}}{V_i + V_o} \tag{6}$$

where

$\Delta v = V_i - V_o$
$m\Delta v$ = change in linear momentum
k_1 = is defined as above

Equation 6 can also be expressed as

$$m\Delta v = \frac{k_1 \frac{V_i}{V_o}}{1 + V_i/V_o} V_i \tag{7}$$

Figure 17 shows that the ratio of impact to exit velocity as a function of impact velocity appears to be constant for 1/16 and 1/8-inch targets, but varies for 1/4-inch targets. Substituting the correct ratio for V_i to V_o from Fig. 17 into Eq. 7 and solving for k_1, the change in linear momentum for 1/16- and 1/8-inch targets was found to be approximately given by:

<u>1/16-inch</u> $$m\Delta v \approx (0.58 \times 10^{-5})\, V_i \tag{8}$$

<u>1/8-inch</u> $$m\Delta v \approx (1.22 \times 10^{-5})\, V_i \tag{9}$$

The linear momentum change for 1/4-inch targets was found to be approximately given by

$$m\Delta v \approx \frac{2.23 \times 10^{-5}\, V_i/V_o}{1 + V_i/V_o} V_i \tag{10}$$

The change in linear momentum as a function of impact velocity is shown in Fig. 18.

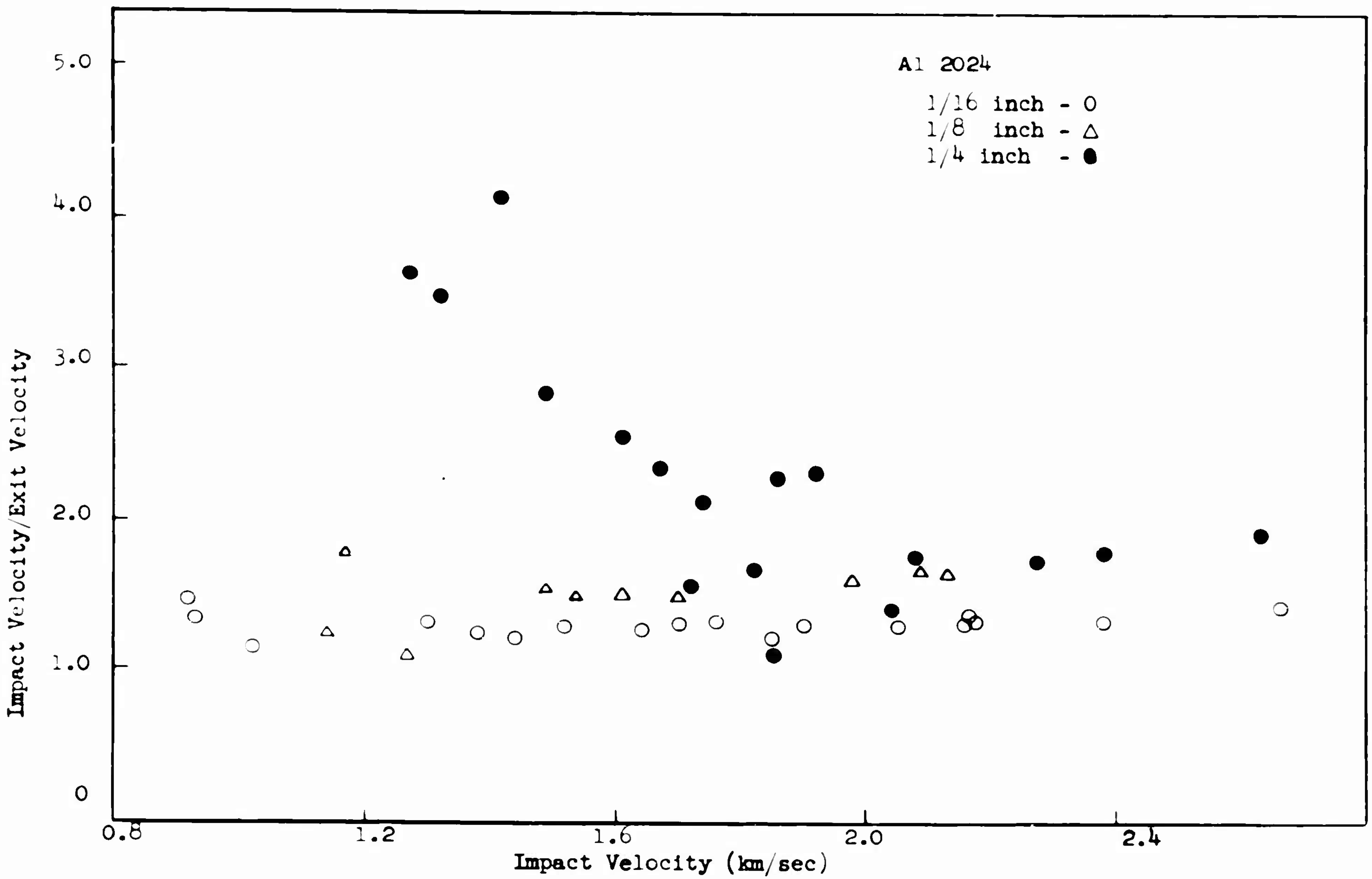

Fig. 17. V_i/V_o vs. impact velocity

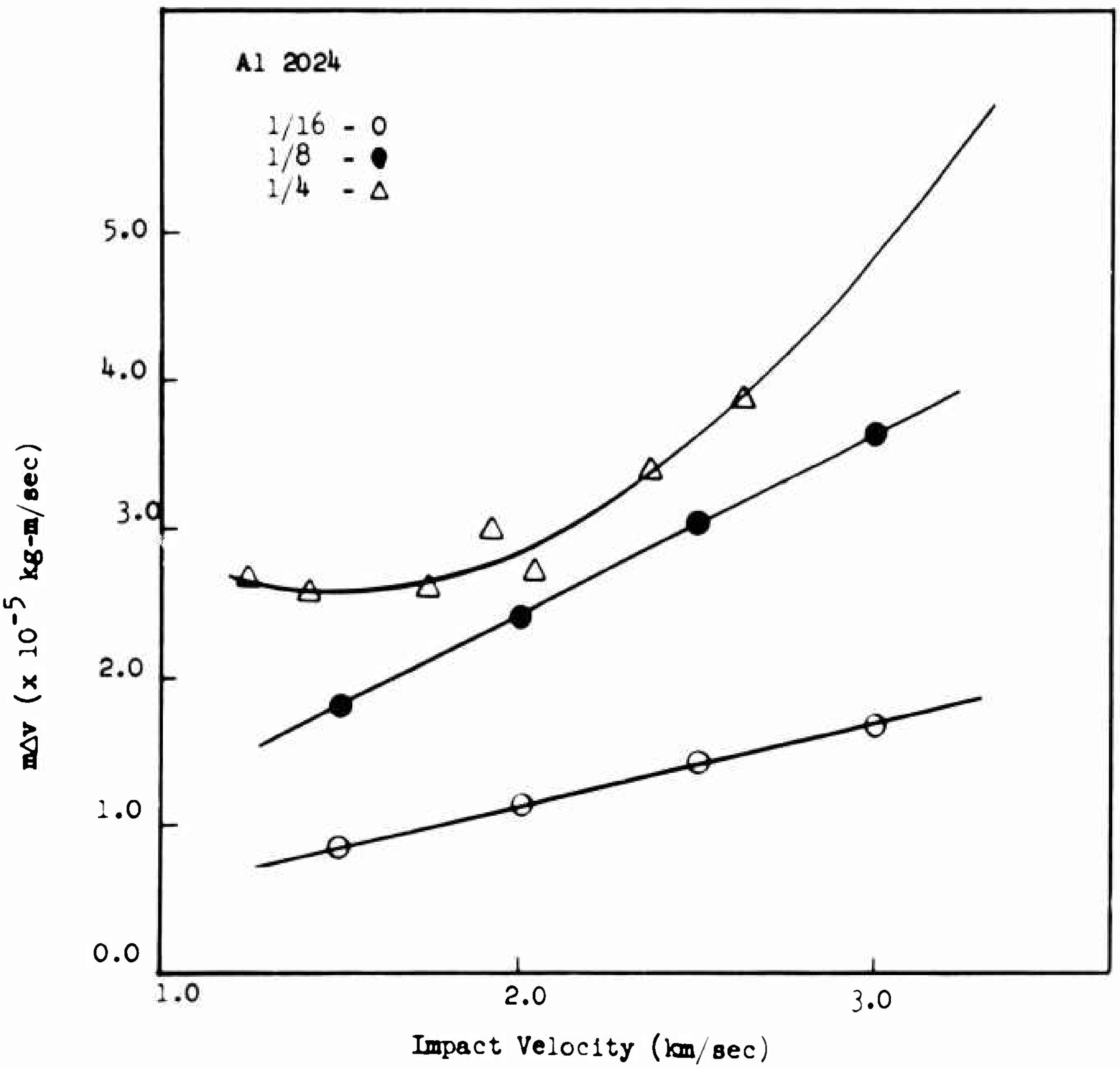

Fig. 18. Momentum change vs. impact velocity

Predicted Loading Condition

An impact load produces a high but finite value which is followed immediately by a rapid decrease. An attempt is made here to predict how this **maximum** finite value varies as a function of impact velocity.

Assume that the force on the target due to the pellet is described by some function of time and velocity as $F = A\,F(v,t)$ where A is the maximum value of F at time $t = 0$. For discussion purposes, assume that $F(v,t)$ decreases very rapidly with time. If it takes a time T_1 for the pellet to perforate a target, then from mechanics the linear impulse equals the change in linear momentum given by:

$$A \int_0^{T_1} F(v,t)\,dt = m\Delta v \qquad (11)$$

where

A = maximum value of F at time $t = 0$

$m\Delta v$ = linear change in momentum of the pellet

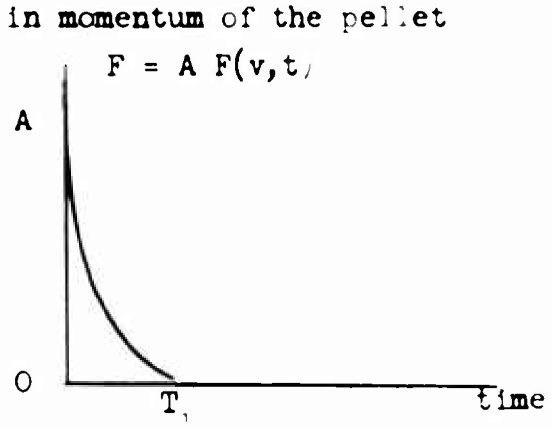

Fig. 19. Approximate curve of force on target

For a given impact velocity, the change in linear momentum can be found by using Fig. 18. The actual time for perforation could be found

quite easily, but for purposes of analysis only, it is sufficient to know that as impact velocity is increased, the perforation time will decrease.

If impact velocity is increased, Fig. 18 indicates there will be an increase in the change of linear momentum. An increase in the change of linear momentum means the area under the curve F in Fig. 19 also increases by Eq. 11. Since the time for perforation decreases for an increasing impact velocity, Fig. 20 shows that the maximum value of F will have to increase from A_1 to A_2 as the perforation time decreases from T_1 to T_2 in order for the integral of F from time t = 0 to time $t = T_2$ to give the correct area.

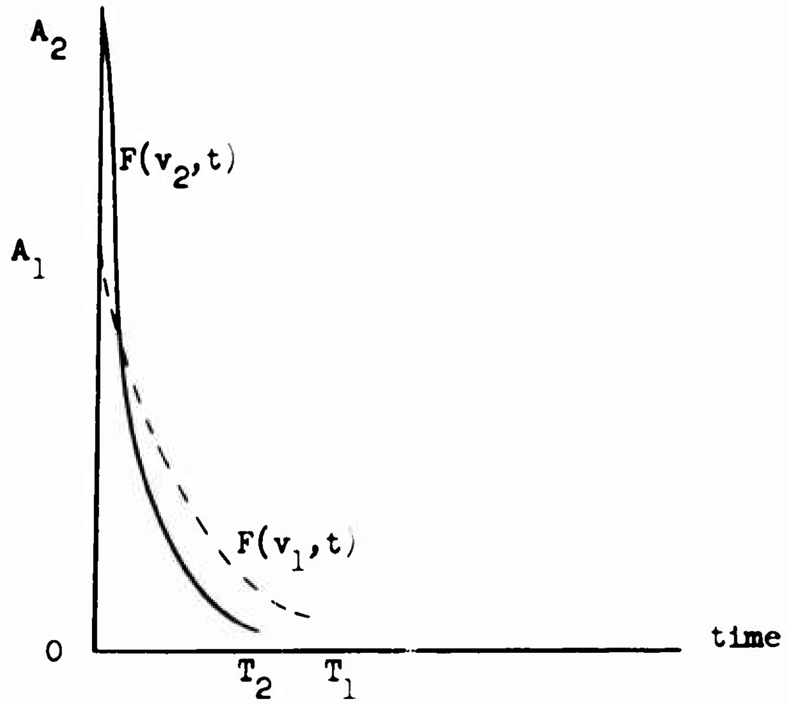

Fig. 20. Theoretical change in maximum load on target as impact velocity increases.

Therefore, the maximum load which appears on the target, although not a function of time is definitely an increasing function of impact velocity.

Predicted Shear Energy

Marks has stated that experiments have shown it takes approximately half as much energy to shear dynamically as it does statically[7]. If this statement is correct, then the shear energy as a function of target thickness is approximately given as shown in Fig. 22*.

Figure 21 shows a photograph of a punchout which was caught from a 1/16-inch target. This punchout shows almost perfect shear. Several such punchouts from 1/16-inch targets were caught and weighed. The mass of a 1/16-inch alumimum punchout having a diameter the same size as the pellet was found to be approximately 10 milligrams.

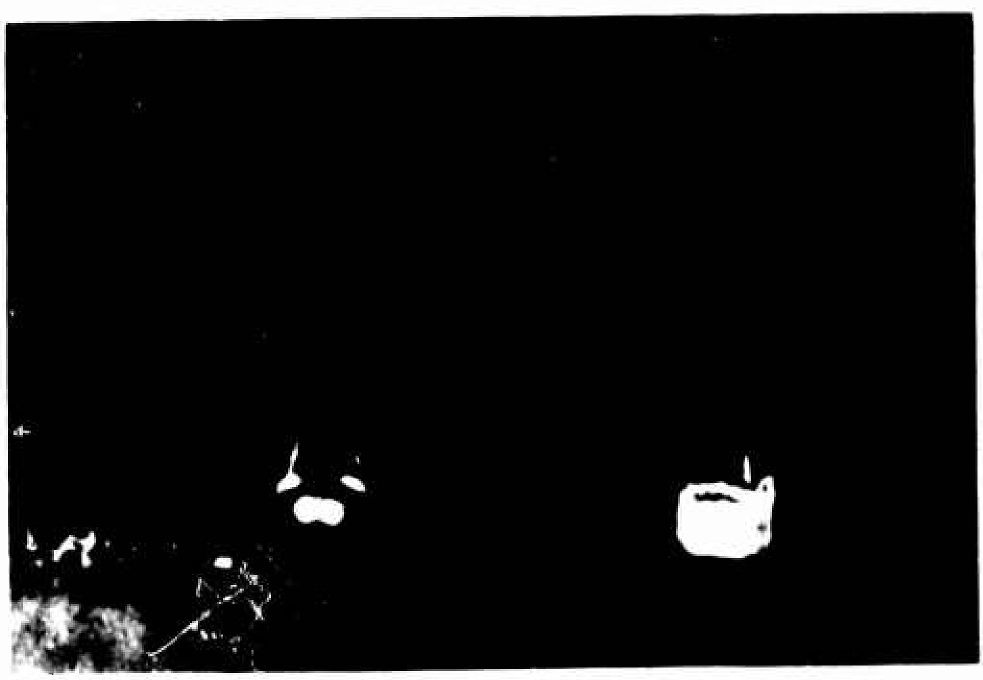

Fig. 21. Punchout showing almost perfect shear and steel pellet

[7] Marks, L. S. "Mechanical Engineers Handbook", Fifth Edition, p. 419, McGraw-Hill Publishers.

* See appendix for calculations.

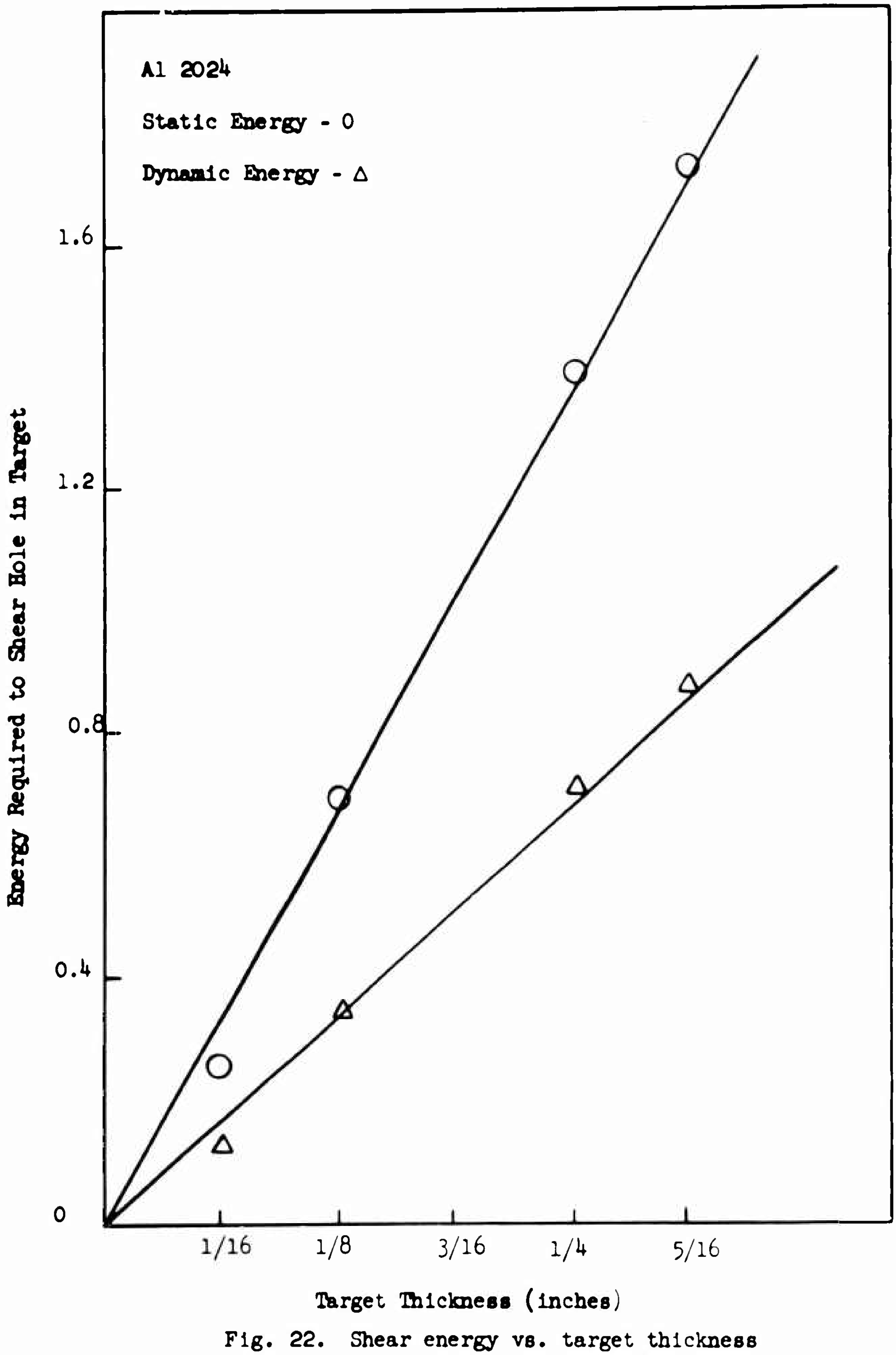

Fig. 22. Shear energy vs. target thickness

SUMMARY

It has been found that the energy lost by a pellet in thin aluminum targets is directly proportional to the kinetic energy of the pellet. The minimum energy of perforation was found to be an increasing function of target thickness.

The size of the hole was found to increase as the energy of the pellet was increased. This checks with Whited's report on crater formation. It was found that the change in linear momentum increased linearly for 1/16- and 1/8-inch targets as impact velocity was increased. The mass of the pellet was found to be constant after perforating the target up to 2.0 km/sec. Between 2.0 and 2.5 km/sec the pellet begins to disintegrate. This was verified by weighing pellets which had perforated targets.

Two theoretical predictions were made. First, the maximum load on the target due to the impinging pellet is an increasing function of impact velocity. Second, the required amount of energy necessary to cause shear of a punchout, being the same size in diameter as the pellet, is approximately one half that of static shearing and increases linearly as target thickness increases.

APPENDIX

The data for the various curves are compiled here. With the chart number will be given the figure for which the data are drawn into a curve.

TABLE I

A. **Material:** Al 2024-T4, 1/16-inch thick

B. **Data:**

Round No.	Striking Time (μsec)	Exit Time (μsec.)
1	544	812
2	628	949
3	542	799
4	361	451
5	347	418
6	359	435
7	337	436
8	328	420
9	334	388
10	244	310
11	356	375
12	230	297
19	386	508
20	537	804
21	542	813
22	564	860
23	778	6,045
24	---	---
25	1,201	---
26	232	303
27	263	337
28	504	947
29	383	520
30	284	368
31	306	382
32	308	586
33	380	503
34	364	462
35	534	694
36	736	1,299
37	---	---
38	260	370
39	295	380
40	340	440
41	260	310
42	190	270
43	210	280
44	230	310
45	290	380
46	270	320
47	520	950
48	540	740
49	440	590
50	490	555

TABLE II

A. **Material:** Al 2024-T4, 1/8-inch thick.

B. **Data:**

Round No.	Striking Time (μsec)	Exit Time (μsec)
1	428	767
2	864	1,072
3	812	933
4	548	6,328
5	437	546
6	455	530
7	239	399
8	235	390
9	230	388
10	393	421
11	253	403
12	294	451
13	324	486
14	310	477
15	335	526
16	342	534
17	341	524
18	348	541
19	305	430
20	300	400
21	300	450
22	240	400
23	255	410
24	240	390
25	260	400
26	260	400
27	340	440
28	320	475
29	340	430
30	480	840
31	780	0
32	600	0
33	550	0
34	610	0
35	660	0
36	690	0
37	300	460
38	240	370
39	230	480
40	240	390
41	240	370
42	225	455
43	220	365

TABLE III

A. Material: Al 2024-T4, 1/4-inch thick

B. Data:

Round No.	Striking Time (μsec)	Exit Time (μsec)
1	352	1,471
2	336	941
3	380	1,277
4	487	0
5	283	587
6	408	2,405
7	269	604
8	287	610
9	402	11,941
10	393	1,447
11	260	600
12	310	800
13	300	710
14	290	460
15	275	465
16	245	345
17	270	300
18	210	380
19	190	370
20	220	390
21	417	0
22	609	0
23	892	0
24	477	0
25	416	0

TABLE IV

A. **Material:** Al 2024-T4, 5/16-inch thick.

B. **Data:**

Round No.	Striking Time (μsec)	Exit Time (μsec)
1	687	0
2	396	0
3	312	0
4	446	0
5	293	--
6	286	0
7	255	--
8	268	--

TABLE V

A. **Material:** Al 2024-T4, 1/2-inch thick.

B. **Data:**

Round No.	Striking Time (μsec)	Exit Time (μsec)
1	248	0
2	235	0
3	277	0
4	285	0
5	200	0

Chart 1 (Figure 4)

Note: All velocities are in km/sec and energy in joules

Rd. No.	V_{in}	V^2_{in}	E_{in}	V_{out}	V^2_{out}	E_{out}	E_{lost}
1	0.92	0.84	23.1	0.62	0.38	10.4	12.7
2	0.80	0.64	17.6	0.53	0.28	7.6	10.0
3	0.92	0.85	23.4	0.63	0.39	10.8	12.6
4	1.38	1.90	52.3	1.11	1.23	33.9	18.4
5	1.44	2.07	57.0	1.19	1.42	39.0	18.0
6	1.39	1.93	53.0	1.15	1.32	36.3	17.0
7	1.48	2.19	60.2	1.15	1.32	36.3	24.0
8	1.52	2.31	63.5	1.19	1.42	39.0	25.0
9	1.49	2.22	61.0	1.29	1.66	45.7	15.0
10	2.05	4.20	115.0	1.61	2.59	71.2	44.0
11	1.41	1.98	54.5	1.33	1.77	48.7	5.0
12	2.18	4.75	130.0	1.68	2.82	77.5	52.0
19	1.30	1.69	46.5	0.98	0.96	26.4	20.1
20	0.93	0.86	23.6	0.62	0.38	10.5	13.1
21	0.92	0.85	23.4	0.62	0.38	10.5	12.9
22	0.89	0.79	21.7	0.58	0.34	9.4	12.3
23	0.64	0.41	11.3	0.08	0.01	0.8	10.5
24	----	----	----	----	----	----	----
25	0.42	----	----	----	----	----	----
26	2.16	4.66	128.0	1.65	2.72	74.6	53.4
27	1.90	3.60	98.0	1.48	2.19	60.2	38.0
28	0.98	0.96	25.4	0.53	0.28	7.6	18.8
29	1.30	1.69	46.5	0.96	0.92	25.3	21.2
30	1.76	3.10	85.4	1.35	1.82	50.0	35.4
31	1.64	2.69	71.3	1.31	1.72	47.3	24.0
32	1.62	2.62	69.4	0.85	0.72	19.8	49.6
33	1.31	1.71	47.0	0.98	0.96	26.4	20.6
34	1.38	1.90	52.3	1.08	1.17	32.2	20.1
35	0.94	0.88	24.2	0.72	0.52	14.3	9.9
36	0.68	0.46	12.7	0.38	0.15	4.1	8.6
37	----	----	----	----	----	----	-----
38	1.92	3.69	101.0	1.35	1.82	50.0	51.0
39	1.70	2.89	79.5	1.32	1.74	47.8	31.7
40	1.47	2.16	59.4	1.14	1.30	35.7	23.7
41	1.92	3.68	101.0	1.62	2.62	72.0	29.0
42	2.63	6.92	190.0	1.85	3.42	94.0	96.0
43	2.38	5.66	155.0	1.79	3.20	88.0	67.0
44	2.18	4.75	130.0	1.62	2.62	72.0	58.0
45	1.72	2.96	82.0	1.32	1.74	47.9	34.1
46	1.85	3.42	94.0	1.56	2.44	67.0	27.0
47	0.96	0.92	25.3	0.53	0.28	7.7	17.6
48	0.93	0.86	23.6	0.68	0.46	12.6	11.0
49	1.14	1.30	35.7	0.85	0.72	19.8	15.9
50	1.02	1.04	28.6	0.90	0.81	22.3	6.3

Chart 2 (Figure 5)

Rd. No.	V_{in}	V^2_{in}	E_{in}	V_{out}	V^2_{out}	E_{out}	E_{lost}
1	1.17	1.37	37.7	0.65	0.43	11.8	25.9
2	0.58	0.34	9.2	0.47	0.22	6.1	3.1
3	0.62	0.38	10.4	0.54	0.28	8.0	2.4
4	0.91	0.83	22.8	0.08	0.01	0.0	----
5	1.14	1.30	38.8	0.92	0.84	23.1	12.7
6	1.10	1.21	33.3	0.94	0.88	24.2	9.1
7	2.09	4.37	120.0	1.25	1.56	42.6	77.2
8	2.13	4.54	125.0	1.28	1.64	45.0	80.0
9	2.17	4.70	129.0	1.29	1.68	46.2	83.0
10	1.27	1.61	44.3	1.18	1.39	38.2	6.1
11	1.98	3.92	108.0	1.24	1.54	42.3	65.7
12	1.70	2.89	79.5	1.11	1.23	33.8	45.7
13	1.54	2.37	65.2	1.03	1.06	29.2	36.0
14	1.61	2.60	71.5	1.04	1.09	30.0	42.0
15	1.49	2.22	61.0	0.95	0.90	24.8	36.0
16	1.46	2.13	58.5	0.94	0.88	24.2	34.3
17	1.47	2.16	59.5	0.96	0.92	25.3	34.2
18	1.43	2.04	56.0	0.93	0.86	23.6	32.4
19	1.64	2.69	74.0	1.16	1.35	37.0	37.0
20	1.67	2.69	77.0	1.25	1.56	42.9	34.0
21	1.67	2.79	77.0	1.11	1.23	33.8	43.2
22	2.08	4.33	119.0	1.25	1.56	43.0	76.0
23	1.96	3.84	105.0	1.22	1.49	41.0	64.0
24	2.08	4.33	119.0	1.28	1.64	45.0	74.0
25	1.92	3.69	101.5	1.25	1.56	43.0	58.5
26	1.92	3.69	101.5	1.25	1.56	43.0	58.5
27	1.47	2.16	59.3	1.13	1.28	35.2	24.1
28	1.56	2.44	67.1	1.05	1.10	30.2	36.9
29	1.47	2.16	59.3	1.16	1.35	37.1	22.2
30	1.04	1.08	29.7	0.60	0.36	9.9	19.8
31	0.64			0.0			
32	0.84			0.0			
33	0.91			0.0			
34	0.82			0.0			
35	0.76			0.0			
36	0.72			0.0			
37	1.67	2.79	76.6	1.09	1.19	32.7	43.9
38	2.08	4.33	119.0	1.35	1.82	50.0	69.0
39	2.18	4.75	130.0	1.04	1.08	29.7	100.3
40	2.08	4.33	119.0	1.28	1.64	45.0	74.0
41	2.08	4.33	119.0	1.35	1.82	50.0	69.0
42	2.22	4.93	135.5	1.10	1.21	33.2	102.3
43	2.27	5.15	141.5	1.37	1.88	51.6	89.9

Chart 3 (Figure 6)

Rd. No.	V_{in}	V^2_{in}	V_{out}	V^2_{out}	$V^2_{in}-V^2_{out}$	E_{lost}
1	1.42	2.02	0.34	0.12	1.90	52.2
2	1.49	2.22	0.53	0.28	1.94	53.3
3	1.32	1.74	0.38	0.14	1.60	44.0
4	1.02	1.04	0.0	0.0	1.04	28.6
5	1.77	3.14	0.85	0.72	2.42	66.5
6	1.22	1.49	0.21	0.04	1.45	40.0
7	1.86	3.46	0.82	0.67	2.79	77.0
8	1.74	3.03	0.82	0.67	2.36	67.0
9	1.24	1.54	0.04	0.00	1.54	42.3
10	1.27	1.61	0.35	0.12	1.49	41.0
11	1.92	3.70	0.83	0.69	3.01	82.6
12	1.61	2.60	0.63	0.39	2.21	61.0
13	1.67	2.80	0.61	0.51	2.29	63.0
14	1.72	2.96	1.09	1.19	1.77	48.7
15	1.82	3.31	1.08	1.17	2.14	58.8
16	2.04	4.16	1.45	2.10	2.06	56.6
17	1.85	3.42	1.67	2.79	0.63	17.3
18	2.38	5.66	1.32	1.74	3.92	107.5
19	2.63	6.91	1.35	1.82	5.09	140.0
20	2.27	5.15	1.28	1.64	3.51	96.5

Chart 4 (Figure 13)

Rd. No.	V_{in}	Hole Entrance Dia.	Hole Exit Dia.	Ratio
21	1.61	0.38	0.25	1.52
17	1.85	0.43	0.28	1.54
19	2.63	0.52	0.47	1.1
15	1.82	0.33	0.24	1.38

Chart 5 (Figure 14)

Rd. No.	V_{in}	Pellet Thickness	Hole Dia.
38	1.92	0.22	0.27
41	1.93	0.21	0.29
42	2.63	0.18	0.33
44	2.18	0.20	****
46	1.85	0.22	0.34
47	0.96	0.24	0.24
48	0.93	0.23	0.24
49	1.14	0.23	0.23
50	1.02	0.21	0.24
51	0.70	0.24	0.24
52	0.59	0.24	0.23
53	0.66	0.24	0.24

Calculations for Nomograph in Figure 15

A standard form was used for parallel and non-equidistant lines. This is given by:

$$F_3\ (c) = F_1(a) + F_2(b)$$

$$\Delta = \begin{vmatrix} -m & Km\ F_1(a) & 1 \\ n & Kn\ F_2(b) & 1 \\ 0 & Kmn\ F_3(c) & m + n \end{vmatrix}$$

By the method of least squares, the coefficient of the curves in Figs. 4, 5, and 6 was found to be a function of target thickness by

$$K = 11.4 + 36.8\ T \qquad (1)$$

Substituting Eq. 1 for K, the amount of energy lost as a function of impact velocity is given by

$$E_{lost} = (11.4 + 36.8\ T)\ V_i^{\ 2} \qquad (2)$$

Taking the log of both sides and relating this to the general, the determinant becomes

$$\Delta = \begin{vmatrix} -m & K\ \overset{(x)}{\overline{\mathrm{Log}(11.4}}\quad \overset{(y)}{\overline{36.8\ T)}} & 1 \\ n & 2K\ \mathrm{Log}\ V_i & 1 \\ 0 & \frac{K}{2}\ \mathrm{Log}\ E_{lost} & 1 \end{vmatrix}$$

By choosing m = 9 and n = 1, the scales were best. The arbitrary constant K was chosen to equal 2.

The nomograph was then made.

Chart 6 (Figure 17)

1/16 inch

Rd. No.	V_{in}	V_{out}	V_{in}/V_{out}
1	0.92	0.62	1.48
4	1.38	1.11	1.24
5	1.44	1.19	1.21
8	1.52	1.19	1.28
10	2.05	1.61	1.27
12	2.18	1.68	1.30
19	1.30	0.98	1.33
26	2.16	1.65	1.31
27	1.90	1.48	1.28
30	1.76	1.35	1.30
31	1.64	1.31	1.25
39	1.70	1.32	1.29
42	2.63	1.85	1.42
43	2.38	1.69	1.33
44	2.18	1.62	1.34
46	1.85	1.56	1.18
48	0.93	0.68	1.37
50	1.02	0.90	1.14

1/8 inch

Rd. No.	V_{in}	V_{out}	V_{in}/V_{out}
1	1.17	0.65	1.80
2	0.58	0.47	1.24
5	1.14	0.92	1.24
7	2.09	1.25	1.67
8	2.13	1.28	1.66
10	1.27	1.18	1.08
11	1.98	1.24	1.60
12	1.70	1.11	1.53
13	1.54	1.03	1.50
14	1.61	1.04	1.55
15	1.49	0.95	1.57

1/4 inch

Rd. No.	V_{in}	V_{out}	V_{in}/V_{out}
1	1.42	0.34	4.17
3	1.32	0.38	3.47
5	1.77	0.85	2.08
6	1.22	0.21	5.80
7	1.86	0.82	2.27
10	1.27	0.35	3.63
11	1.92	0.83	2.32
12	1.61	0.63	2.56
14	1.72	1.09	1.58
16	2.04	1.45	1.41
17	1.85	1.67	1.11
18	2.38	1.32	1.80
19	2.63	1.35	1.95
20	2.27	1.28	1.77

Calculations for Shear Energy (Figure 20)

For aluminum 2024, Modulus of Toughness = 4,040 $\frac{\text{in-lb}}{\text{in}^3}$ (1)

Volume of hole = $\frac{\pi D^2}{4}$ x thickness (2)

Using Eq. 1 and 2, the following was found for static shearing.

Thickness	Vol. of Hole	Energy to Shear
1/16	4.38×10^{-4} in^3	0.343 joules
1/8	8.75×10^{-4} in^3	0.693 joules
1/4	17.5×10^{-4} in^3	1.39 joules
5/16	21.8×10^{-4} in^3	1.73 joules

The dynamic energy was assumed to be half of the static energy.